

## Supplementary Information - Investigating the Effect of Heteroatom Substitution in 2,1,3-Benzoxadiazole and 2,1,3-Benzothiadiazole Compounds for Organic Photovoltaics

Joseph Cameron,<sup>a,†</sup> Mahmoud Matar Abed,<sup>a</sup> Steven J. Chapman,<sup>a</sup> Neil J. Findlay,<sup>a,†</sup> Peter J. Skabara<sup>a,†,\*</sup>, Peter N. Horton<sup>b</sup> and Simon J. Coles<sup>b</sup>

<sup>a</sup>WestCHEM, Department of Pure and Applied Chemistry, University of Strathclyde, G1 1XL, UK;

<sup>b</sup>School of Chemistry, University of Southampton, Highfield, Southampton, SO17 1BJ, UK

<sup>†</sup> New address: School of Chemistry, University of Glasgow, Glasgow G12 8QQ, UK

\*Email: peter.skabara@glasgow.ac.uk

### Contents

General Experimental.....	2
Synthetic procedures for all compounds.....	4
Figure S1: <sup>1</sup> H NMR spectrum of <b>BT-(TBF)<sub>2</sub></b> .....	7
Figure S2: <sup>13</sup> C NMR spectrum of <b>BT-(TBF)<sub>2</sub></b> .....	8
Figure S3: <sup>1</sup> H NMR spectrum of <b>BO-(TBF)<sub>2</sub></b> .....	8
Figure S4: <sup>13</sup> C NMR spectrum of <b>BO-(TBF)<sub>2</sub></b> .....	9
Figure S5: Cyclic voltammograms for <b>BT-(TBF)<sub>2</sub></b> and <b>BO-(TBF)<sub>2</sub></b> .....	9
Figure S6: Crystal packing structure of <b>BT-(TBF)<sub>2</sub></b> viewed along the <i>a</i> -axis.....	10
Figure S7: Crystal packing structure of <b>BO-(TBF)<sub>2</sub></b> viewed along the <i>a</i> -axis.....	11
Figure S8: Output and transfer characteristics for OFETs containing <b>BT-(TBF)<sub>2</sub></b> .....	12
Figure S9: Output and transfer characteristics for OFETs containing <b>BO-(TBF)<sub>2</sub></b> .....	12
Figure S10: <i>J-V</i> characteristics for OPV devices containing <b>BT-(TBF)<sub>2</sub></b> or <b>BO-(TBF)<sub>2</sub></b> .....	13
References.....	13

## Experimental

For all reactions carried out in anhydrous conditions, glassware was dried in an oven at 130°C. Reagents were purchased from commercial sources without further purification unless otherwise stated. Compound **1** was synthesised according to a previously reported procedure.<sup>1</sup> Dry solvents were obtained from a solvent purification system (SPS 400 by Innovative Technologies) with an alumina drying agent. <sup>1</sup>H and <sup>13</sup>C NMR spectra were recorded on DRX 500 or AV3 400 at 500 and 125 MHz or 400 and 100 MHz, respectively. Chemical shifts are in ppm and *J* values are in Hz. Low resolution mass spectrometry (LRMS) was performed on a Shimadzu Axima-CFR spectrometer (MALDI). High resolution mass spectrometry (HRMS) was gratefully performed by the EPSRC National Mass Spectrometry Facility at Swansea. Elemental analyses were performed on a Perkin-Elmer 2400 analyser. Melting points were determined using a Stuart Scientific SMP1 Melting Point apparatus and are uncorrected. Cyclic voltammetry measurements were carried out in order to characterise the HOMO and LUMO levels of each compound. This was performed using a CH Instruments 660A electrochemical workstation with *iR* compensation at a scan rate of 0.1 V s<sup>-1</sup>. The concentration of analyte used was 1×10<sup>-4</sup> M in CH<sub>2</sub>Cl<sub>2</sub> with tetrabutylammonium hexafluorophosphate (0.1 M) used as an electrolyte. Glassy carbon, Ag wire and Pt wire were used as the working, quasi-reference and counter electrodes, respectively. Each value is corrected to the redox potential of ferrocene. The HOMO (LUMO) was calculated by subtracting the peak potential of oxidation (reduction) from -4.8 eV, the HOMO of ferrocene. The UV-vis absorption profile of all compounds was recorded using a Shimadzu UV-1800 spectrophotometer. Solution-state spectroscopy was carried out using 10<sup>-5</sup> M solutions in CH<sub>2</sub>Cl<sub>2</sub> unless otherwise stated, whilst solid-state spectroscopy was carried out by drop-casting a 2 mg ml<sup>-1</sup> toluene solution onto a quartz slide and allowing the solvent to evaporate. The low-energy onset of the longest wavelength absorption band was used in order to calculate the optical HOMO-LUMO gap for each compound.

Organic field-effect transistors were fabricated on SiO<sub>2</sub> substrates with prefabricated interdigitated Au source-drain channels with lengths of 10 and 20 μm and width of 1 cm. N-doped Si and SiO<sub>2</sub> are the gate electrode and gate dielectric respectively. The substrates were cleaned using water, acetone and ethanol before being treated with oxygen plasma cleaning (Diener Electronic, Zepto) for 30 seconds. Octadecyltrichlorosilane (OTS) SAM was prepared by drop-casting an OTS solution (13 mM in toluene) onto the substrate which was washed with toluene and dried after 1 min. **BT-(TBF)<sub>2</sub>** and **BO-(TBF)<sub>2</sub>** (concentration: 10 mg ml<sup>-1</sup> in CHCl<sub>3</sub>) were deposited *via* spin-coating (MB SC-200, MBraun) at 2000 rpm before annealing at a stated temperature. Current-voltage characteristics were recorded using a Keithley 4200

semiconductor parameter analyser at room temperature in a nitrogen atmosphere. Data was averaged over 5 devices. The field-effect mobilities were determined from the saturation

regime and calculated using the following equation:

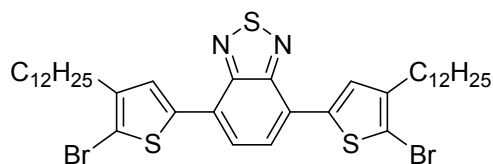
$$\mu_{sat} = \frac{2L}{WC_i} \times \left( \frac{\partial \sqrt{I_{ds}}}{\partial V_g} \right)^2$$

In OPV fabrication, ITO glass slides were cleaned with deionised water, acetone and isopropanol before treatment with UV-ozone for 2 minutes. PEDOT:PSS (Clevios™ P VP AL 4083) was then spin-coated onto the ITO at 3000 rpm and the substrates were then annealed for 20 minutes at 120°C. After the substrates were taken into the glovebox with N<sub>2</sub> atmosphere, the active material (10 mg ml<sup>-1</sup> donor, 20 mg ml<sup>-1</sup> PC<sub>61</sub>BM (Nano-C, 99.5%) in CHCl<sub>3</sub>) was then spin-coated onto the substrate at 800 rpm before being annealed at the stated temperature for 20 minutes. Calcium and aluminium electrodes were then evaporated onto the active layer respectively with thickness of 40 nm for each metal. The area of the electrodes deposited was 6 mm<sup>2</sup>. Active areas of devices were defined by a shadow mask. The current-voltage characteristics were measured using a Keithley 4200 and the solar cells were illuminated by a Newton Solar Simulator with a calibrated solar cell. Data was averaged over 5 devices. Only 2 were averaged for devices containing **BT-(TBF)<sub>2</sub>** as donor with DIO additive due to poor morphology. The surface morphology was characterised using a Dimension 3100 atomic force microscopy (AFM) in tapping mode. The software WSxM 5.0 was used to analyse the images.<sup>2</sup>

Suitable crystals for **BO-(TBF)<sub>2</sub>** and **BT-(TBF)<sub>2</sub>** were selected and data collected following a standard method,<sup>3</sup> on a Rigaku AFC12 goniometer at 100K equipped with an enhanced sensitivity (HG) Saturn724+ detector mounted at the window of an FR-E-Superbright molybdenum anode generator with HF Varimax optics (100µm focus). Cell determination, data collection, data reduction, cell refinement and absorption correction were carried out using CrysAlisPro.<sup>4</sup> Within Olex2,<sup>5</sup> the structures were solved using SHELXT<sup>6</sup> and refinement using SHELXL.<sup>7</sup>

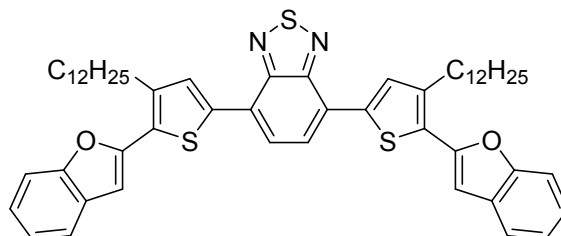
## Synthetic Procedures

### 4,7-Bis(5-bromo-4-dodecylthiophen-2-yl)benzo[c][1,2,5]thiadiazole, (2)



Compound **1** (164 mg, 0.257 mmol) and *N*-bromosuccinimide (112 mg, 0.628 mmol) were dissolved in 10 mL of chloroform and the reaction was allowed to stir for 16 h in the absence of light. The solution was diluted with CH<sub>2</sub>Cl<sub>2</sub> and washed with brine (3 × 50 mL), before being dried with MgSO<sub>4</sub> and the solvent was removed under reduced pressure. The crude material was purified by column chromatography (silica gel, 1:10 CH<sub>2</sub>Cl<sub>2</sub>/hexane eluent) to give the product as a red solid. Yield = 0.128 g (63%). <sup>1</sup>H NMR (400 MHz, CDCl<sub>3</sub>) δ<sub>H</sub> 7.77 (s, 2H), 7.76 (s, 2H), 2.69 – 2.60 (m, 4H), 1.67 (m, 4H), 1.44 – 1.20 (m, 36H), 0.87 (t, *J* = 6.9 Hz, 6H); *m/z* (MALDI): 793.88 [M<sup>+</sup>]; Melting point: 62–64°C. Consistent with previous data.<sup>8</sup>

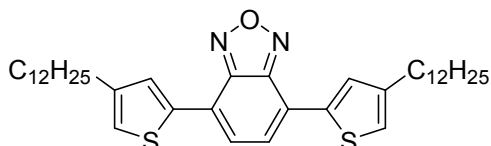
### 4,7-Bis(5-(benzofuran-2-yl)-4-dodecylthiophen-2-yl)benzo[c][1,2,5]thiadiazole, (3), BT-(TBF)<sub>2</sub>



Compound **2** (100 mg, 0.126 mmol), potassium carbonate (52 mg, 0.378 mmol) and 2-benzofuranylboronic acid MIDA ester (85 mg, 0.106 mmol) were added to a flask which was evacuated and purged with argon before the addition of anhydrous THF (4 mL) and degassed H<sub>2</sub>O (0.45 mL). The solution was then allowed to degas for 30 minutes before the addition of Pd(PPh<sub>3</sub>)<sub>4</sub> (15 mg, 0.016 mmol). The reaction mixture was then heated at 70°C for 36 h with stirring. The resulting mixture was cooled to room temperature before being diluted with CH<sub>2</sub>Cl<sub>2</sub>, washed with brine (3 × 50 mL) and dried over MgSO<sub>4</sub> before removal of solvent under reduced pressure. Column chromatography (silica gel, 1:10 CH<sub>2</sub>Cl<sub>2</sub>/hexane eluent) was used to purify the crude material to give the product as a dark red/purple solid. Yield = 0.11 g (76%). <sup>1</sup>H NMR (400 MHz, CDCl<sub>3</sub>) δ<sub>H</sub> 8.02 (s, 2H), 7.88 (s, 2H), 7.59 (dd, *J* = 7.5, 0.8 Hz, 2H), 7.53 (m, 2H), 7.34 – 7.21 (m, 4H), 6.88 (s, 2H), 3.03 – 2.89 (m, 4H), 1.81 (m, 4H), 1.52 – 1.19 (m,

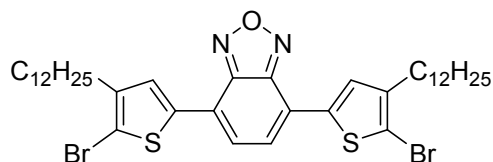
36H), 0.88 (t,  $J = 6.8$  Hz, 6H);  $^{13}\text{C}$  NMR (101 MHz,  $\text{CDCl}_3$ )  $\delta_{\text{C}}$  154.5, 152.7, 151.2, 142.3, 138.4, 130.9, 129.4, 128.6, 126.3, 125.7, 125.5, 124.6, 123.3, 120.9, 111.2, 103.2, 32.1, 30.2, 30.1, 29.9, 29.7, 29.5, 22.8, 14.3;  $m/z$  (MALDI): 868.09  $[\text{M}]^+$ ; anal. calculated for  $\text{C}_{54}\text{H}_{64}\text{N}_2\text{O}_2\text{S}_3$ : C, 74.61, H, 7.42, N, 3.22. Found: C, 74.28, H, 7.33, N, 3.24; Melting point: 90-92°C.

**4,7-Bis(4-dodecylthiophen-2-yl)benzo[c][1,2,5]oxadiazole, (4)**



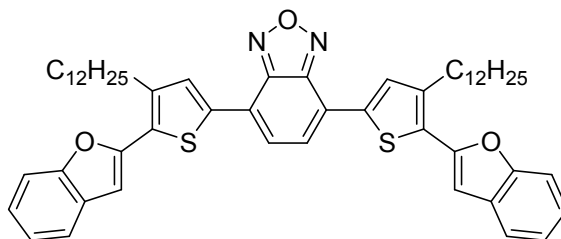
To an oven dried microwave vial, 4,7-dibromo-2,1,3-benzoxadiazole (450 mg, 1.61 mmol) was added followed by  $\text{Pd}(\text{PPh}_3)_4$  (370 mg, 0.32 mmol). The vial was evacuated and purged with argon. 2-Trimethylstannyl-4-dodecylthiophene (2.0 g, 4.82 mmol) was then added followed by anhydrous tetrahydrofuran (2.5 mL). The reaction mixture was degassed using nitrogen gas for 5 min. The vial was sealed and placed in a microwave reactor for 2 h at 100°C. After cooling to room temperature an additional portion of  $\text{Pd}(\text{PPh}_3)_4$  (180 mg, 0.16 mmol) was added. The reaction mixture was then degassed with nitrogen for 5 minutes, and the vial was sealed. The vial was placed in the microwave reactor to stir for an additional 3 h at 100°C. The reaction mixture was cooled to room temperature and diluted with  $\text{CH}_2\text{Cl}_2$  before being washed with deionized water ( $3 \times 100$  mL) and brine ( $1 \times 100$  mL). The organic layer was collected, dried using  $\text{MgSO}_4$  and the solvent was evaporated under reduced pressure. Column chromatography was performed (silica gel, 1:20  $\text{CH}_2\text{Cl}_2$ /Hexane eluent) to yield a red solid. Yield = 591 mg (58 %).  $^1\text{H}$  NMR ( $\text{CDCl}_3$ , 400 MHz)  $\delta_{\text{H}}$  7.97 (s, 2H), 7.57 (s, 2H), 7.04 (s, 2H), 2.69 (t,  $J = 4$  Hz, 4H), 1.71 (d,  $J = 8$  Hz, 4H), 1.32 (m, 36H), 0.89 (t,  $J = 4$  Hz, 6H);  $^{13}\text{C}$  NMR ( $\text{CDCl}_3$ , 100 MHz)  $\delta_{\text{C}}$  147.9, 145.1, 137.6, 130.2, 126.1, 121.9, 121.7, 31.9, 31.8, 30.6, 30.5, 29.7, 29.5, 22.7, 14.1;  $m/z$  (MALDI) 620.42  $[\text{M}]^+$ ; anal. calculated for  $\text{C}_{38}\text{H}_{56}\text{N}_2\text{OS}_2$ : C, 73.50, H, 9.09, N, 4.51. Found: C, 73.46, H, 8.70, N, 4.31; Melting point: 76-77°C.

**4,7-Bis(5-bromo-4-dodecylthiophen-2-yl)benzo[c][1,2,5]oxadiazole, (5)**



To an oven dried two neck flask, compound **3** (400 mg, 0.64 mmol) was dissolved in anhydrous THF and cooled to 0°C. *N*-Bromosuccinimide (239 mg, 1.34 mmol) was then added in one portion. The reaction was stirred at 0°C and gradually warmed to room temperature overnight. The reaction was quenched with a saturated aqueous ammonium chloride solution, extracted with ethyl acetate, washed with water (3 × 100 mL) and dried with MgSO<sub>4</sub> before evaporation of solvent under reduced pressure to give an orange solid. Yield = 387 mg (77 %). <sup>1</sup>H NMR (CDCl<sub>3</sub>, 400 MHz)  $\delta_H$  7.82 (s, 2H), 7.45 (s, 2H), 2.63 (t, *J* = 8 Hz, 4H), 1.68 (d, *J* = 4 Hz, 4H), 1.36 (m, 36H), 0.89 (t, *J* = 4 Hz, 6H); <sup>13</sup>C NMR (CDCl<sub>3</sub>, 100 MHz)  $\delta_C$  147.5, 144.0, 137.1, 129.8, 125.8, 121.49, 111.6, 35.3, 31.9, 29.7, 29.6, 29.4, 29.2, 22.7, 14.1; *m/z* (MALDI) 778.21 [M]<sup>+</sup>; HRMS (APCI, *m/z*) calc. for C<sub>38</sub>H<sub>54</sub>Br<sub>2</sub>N<sub>2</sub>OS<sub>2</sub>, 779.2099 ([M + H]<sup>+</sup>); found, 779.2087 ([M + H]<sup>+</sup>); Melting point: 75-77°C.

**4,7-Bis(5-(benzofuran-2-yl)-4-dodecylthiophen-2-yl)benzo[c][1,2,5]oxadiazole, (6), BO-(TBF)<sub>2</sub>**



4,7-Bis(5-bromo-4-dodecylthiophen-2-yl)-2,1,3-benzoxadiazole (175 mg, 0.225 mmol), potassium carbonate (158 mg, 0.114 mmol) and 2-benzofuranylboronic acid MIDA ester (148 mg, 0.542 mmol) were added to a vial which was subsequently evacuated and purged with argon. Anhydrous THF (10 mL) and degassed water (1 mL) were then added to the vial and the reaction mixture was degassed for 45 minutes using argon. Pd(PPh<sub>3</sub>)<sub>4</sub> (81 mg, 0.070 mmol) was added to the solution and the reaction was carried out in a microwave reactor with stirring at 100°C for 2 h. The solution was diluted with CH<sub>2</sub>Cl<sub>2</sub>, washed with brine (3 × 50 mL), dried over MgSO<sub>4</sub> and the solvent was removed under reduced pressure. The crude material was then purified by column chromatography (silica gel, 1:10 CH<sub>2</sub>Cl<sub>2</sub>/hexane eluent) to give the final product as a red/purple solid. Yield = 138 mg (72 %). <sup>1</sup>H NMR (400 MHz, CDCl<sub>3</sub>)  $\delta_H$  7.97 (s, 2H), 7.60 – 7.54 (m, 4H), 7.54 – 7.48 (m, 2H), 7.29 (m, 2H), 7.26 – 7.21 (m, 2H), 6.86 (d, *J* =

0.7 Hz, 2H), 2.90 (t,  $J = 7.9$  Hz, 4H), 1.78 (m, 4H), 1.52 – 1.20 (m, 36H), 0.88 (t,  $J = 6.9$  Hz, 6H);  $^{13}\text{C}$  NMR (101 MHz,  $\text{CDCl}_3$ )  $\delta_{\text{C}}$  154.4, 150.7, 147.9, 142.8, 136.7, 132.2, 129.2, 128.7, 126.8, 124.8, 123.4, 121.7, 121.0, 111.2, 103.7, 77.5, 77.1, 76.8, 32.1, 30.2, 29.9, 29.83, 29.79, 29.6, 29.5, 22.8, 14.3;  $m/z$  (MALDI): 852.36  $[\text{M}]^+$ ; anal. calculated for  $\text{C}_{54}\text{H}_{64}\text{N}_2\text{O}_3\text{S}_2$ : C, 76.02, H, 7.56, N, 3.28. Found, C, 75.98, H, 7.56, N, 3.33. Melting point 112-114°C.

## NMR Spectra

Person 7-1  
MA006 F  
@proton  $\text{CDCl}_3$  {C:\NMRdata} pjs 61

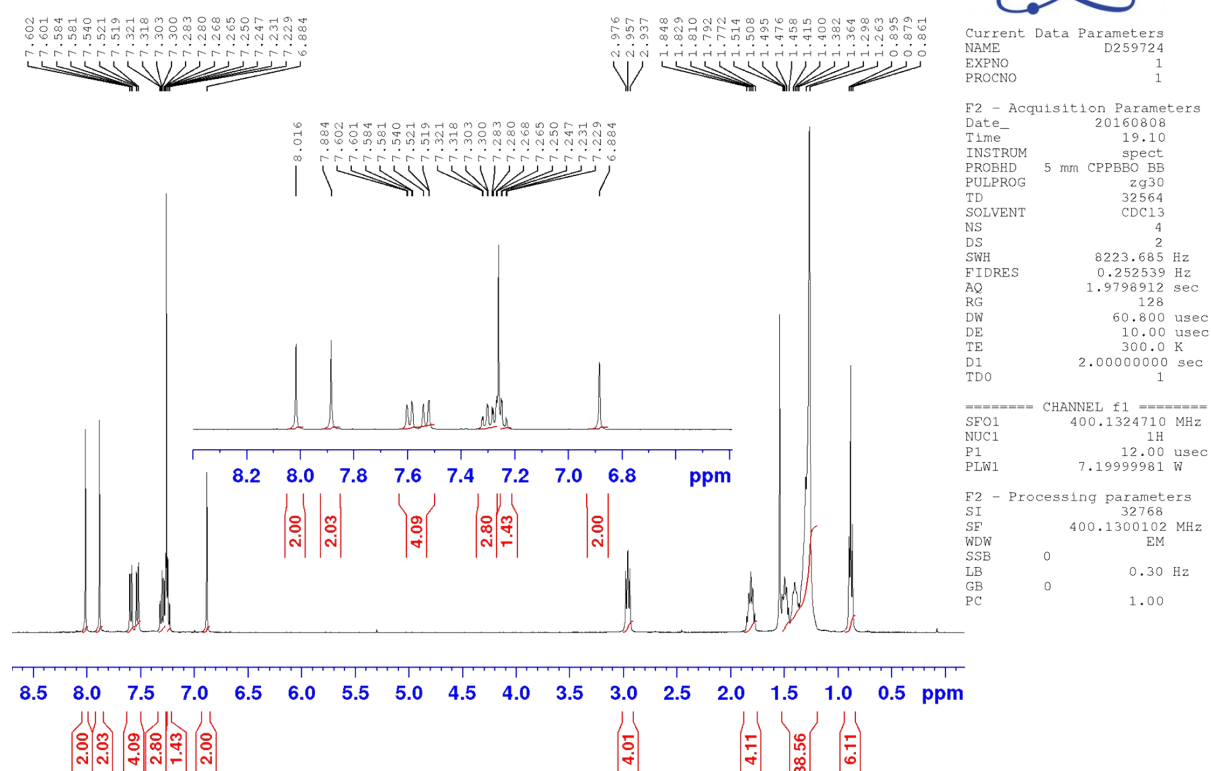


Figure S1.  $^1\text{H}$  NMR of  $\text{BT}-(\text{TBF})_2$

Person 7-1  
MA006 F  
13C\_@ CDC13 {C:\NMRdata} pjs 61

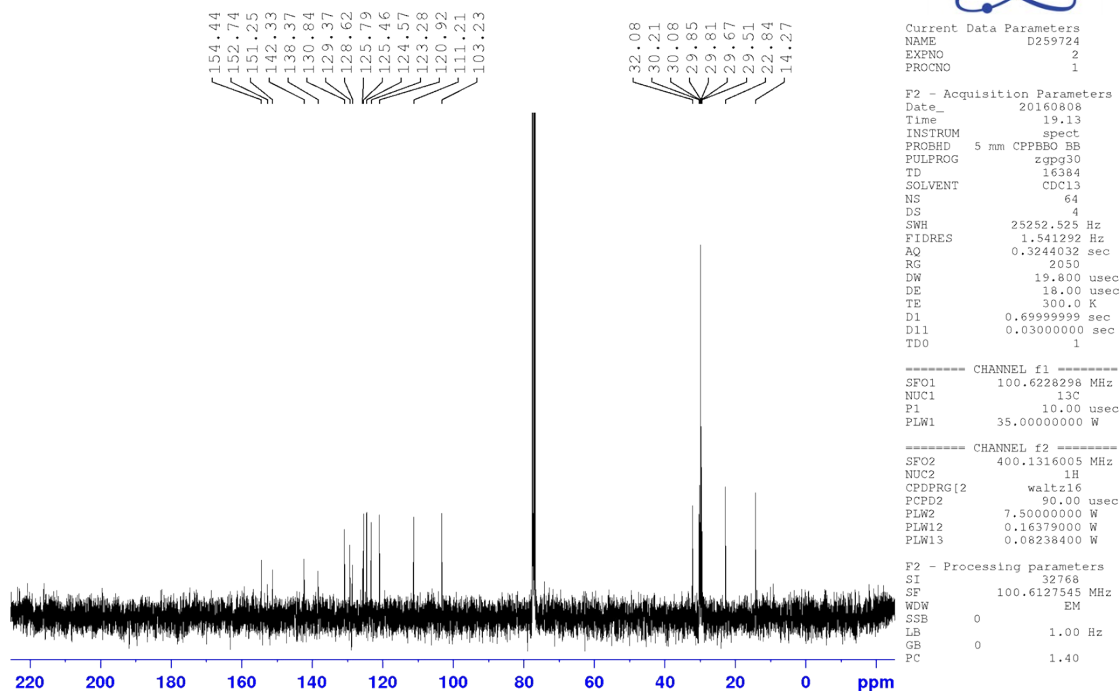


Figure S2.  $^{13}\text{C}$  NMR of BT-(TBF) $_2$

Person 7-1  
MA007 F  
@proton CDC13 {C:\NMRdata} pjs 62

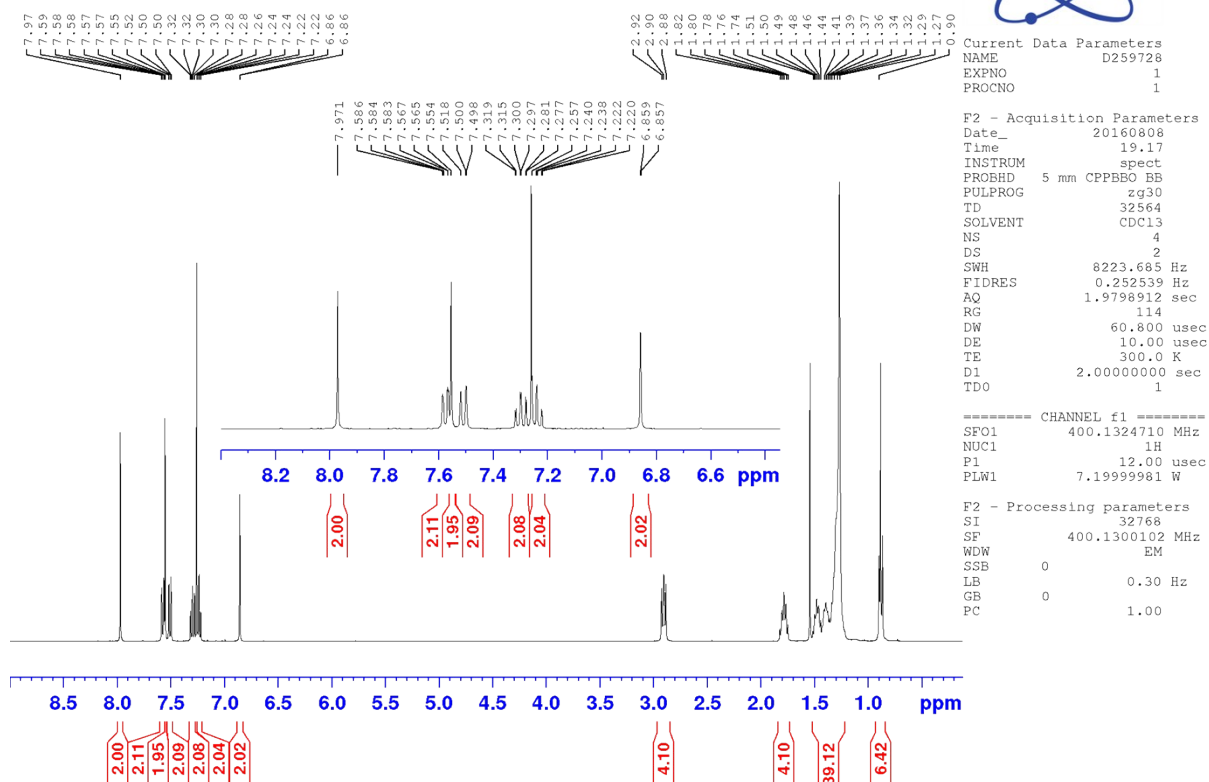


Figure S3.  $^1\text{H}$  NMR of BO-(TBF) $_2$



Person 7-1  
MA007 F  
13C\_@ CDC13 {C:\NMRdata} pjs 62

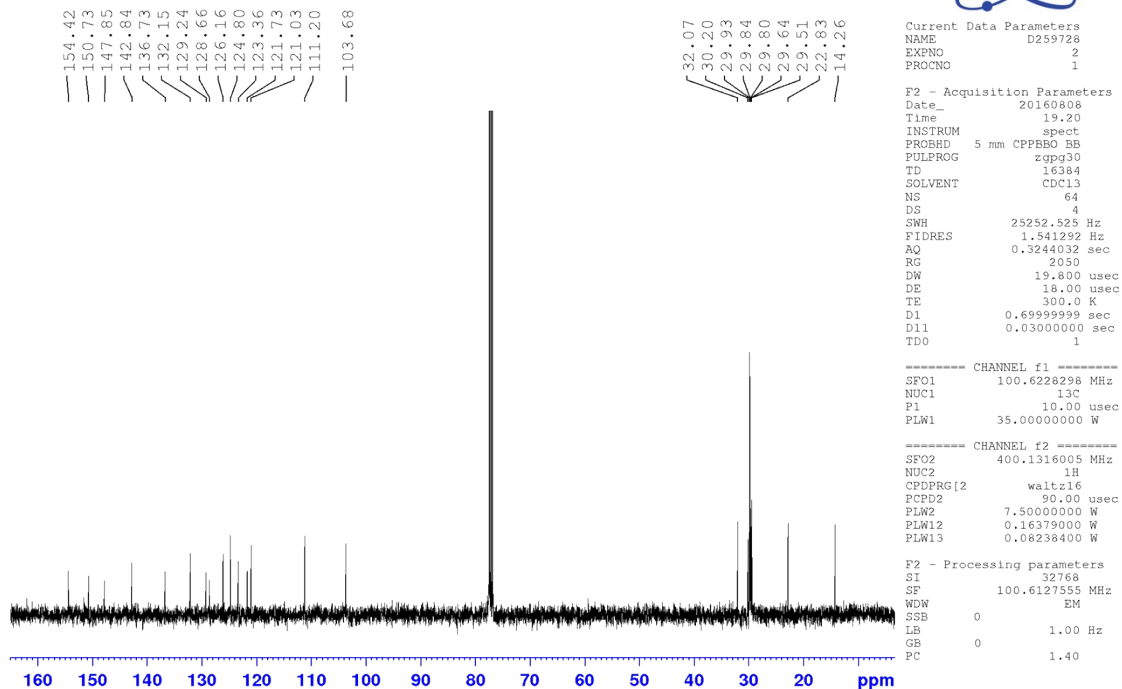


Figure S4.  $^{13}\text{C}$  NMR of  $\text{BO}-(\text{TBF})_2$

### Cyclic Voltammetry

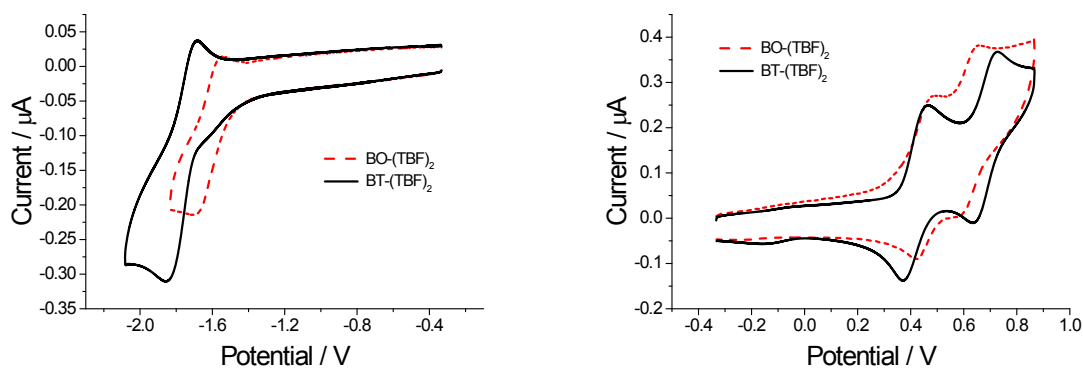
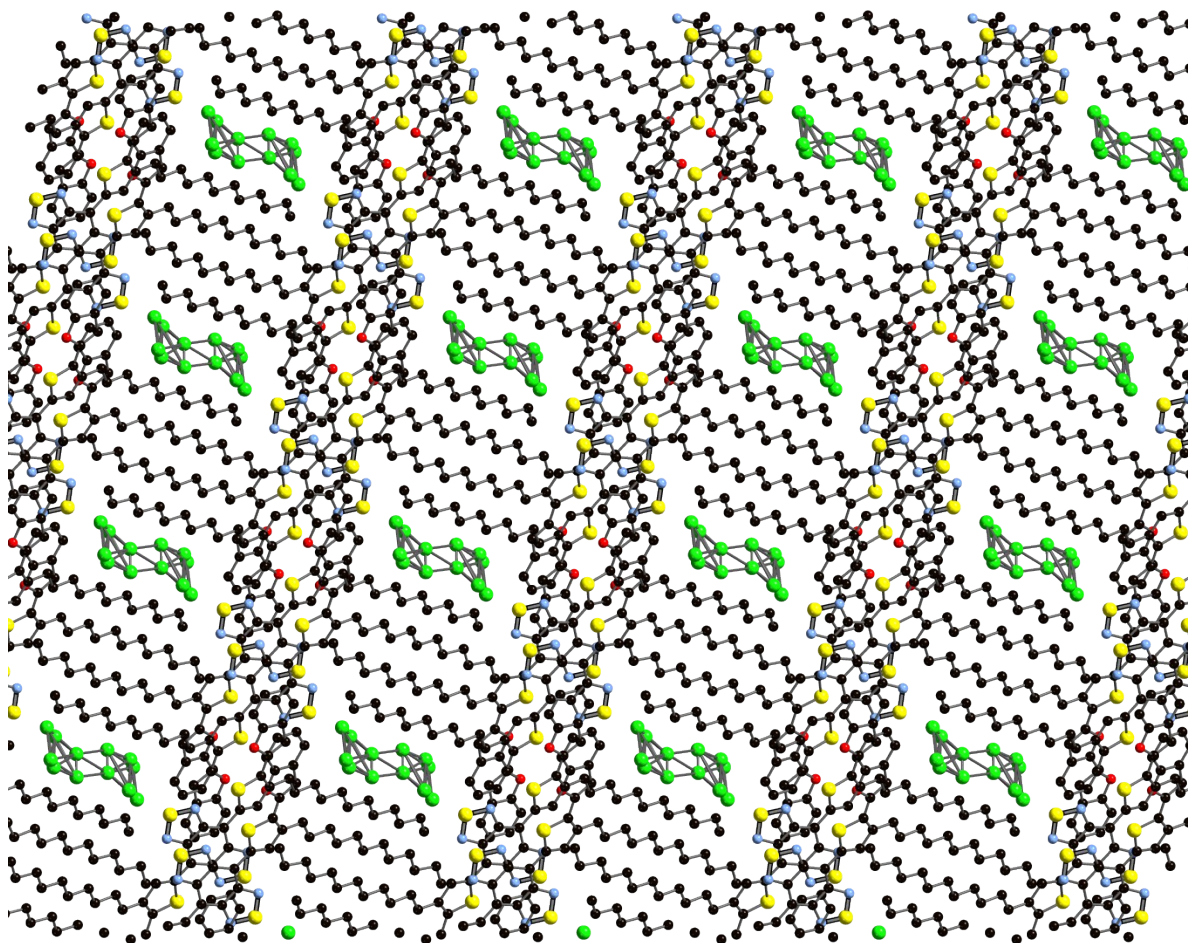


Figure S5. Reduction (left) and oxidation (right) of  $\text{BT}-(\text{TBF})_2$  and  $\text{BO}-(\text{TBF})_2$  by cyclic voltammetry

## X-Ray Crystallography



**Figure S6.** Crystal packing structure of **BT-(TBF)<sub>2</sub>** viewed along the *a*-axis.

Crystal data for **BT-(TBF)<sub>2</sub>** :  $\text{C}_{55}\text{H}_{65}\text{Cl}_3\text{N}_2\text{O}_2\text{S}_3$ ,  $M_r = 988.62$ , dark red plate, triclinic, space group *P*-1,  $a = 11.6431(6) \text{ \AA}$ ,  $b = 13.1881(11) \text{ \AA}$ ,  $c = 18.3509(12) \text{ \AA}$ ,  $\alpha = 72.963(6)^\circ$ ,  $\beta = 76.859(5)^\circ$ ,  $\gamma = 76.620(6)^\circ$ ,  $V = 2582.2(3) \text{ \AA}^3$ ,  $T = 100(2) \text{ K}$ ,  $Z = 2$ ,  $Z' = 1$ ,  $\mu(\text{MoK}\alpha) = 0.341$ , 52160 reflections measured, 11647 unique ( $R_{\text{int}} = 0.0527$ ).  $R1 = 0.0946$ ,  $wR2 = 0.1875$  [ $F^2 > 2\sigma(F^2)$ ],  $R1 = 0.1168$ ,  $wR2 = 0.1983$  (all data).

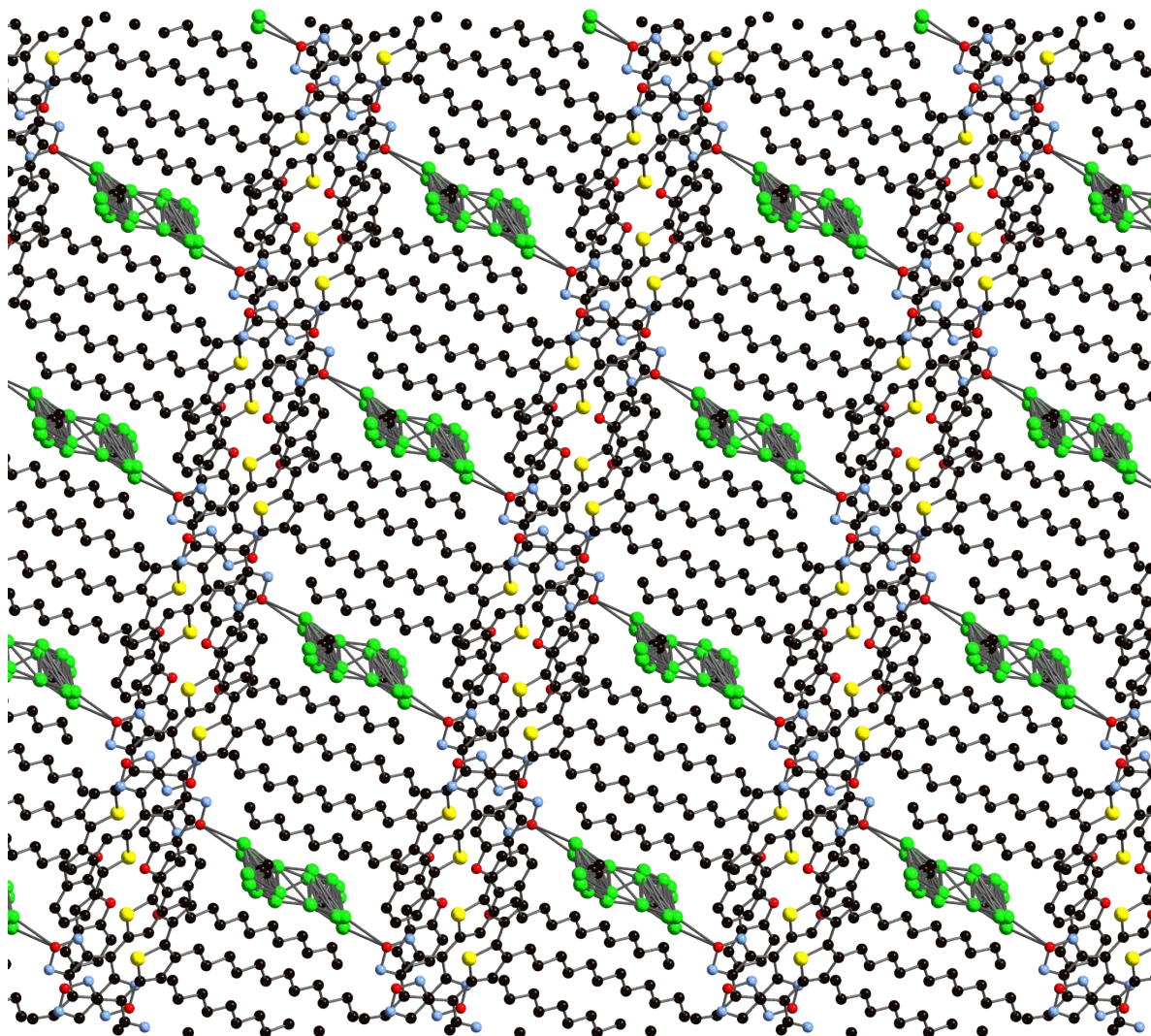


**Figure S7.** Crystal packing structure of **BO-(TBF)<sub>2</sub>** viewed along the *a*-axis.

Crystal data for **BO-(TBF)<sub>2</sub>** : C<sub>55</sub>H<sub>65</sub>Cl<sub>3</sub>N<sub>2</sub>O<sub>3</sub>S<sub>2</sub>,  $M_r = 972.56$ , red plate, triclinic, space group *P*-1,  $a = 11.6310(2) \text{ \AA}$ ,  $b = 12.9034(4) \text{ \AA}$ ,  $c = 18.3333(5) \text{ \AA}$ ,  $\alpha = 72.595(2)^\circ$ ,  $\beta = 77.433(2)^\circ$ ,  $\gamma = 77.292(2)^\circ$ ,  $V = 2526.88(12) \text{ \AA}^3$ ,  $T = 100(2) \text{ K}$ ,  $Z = 2$ ,  $Z' = 1$ ,  $\mu(\text{MoK}\alpha) = 0.309$ , 55199 reflections measured, 11551 unique ( $R_{\text{int}} = 0.0538$ ).  $R1 = 0.0518$ ,  $wR2 = 0.1260$  [ $F^2 > 2\sigma(F^2)$ ],  $R1 = 0.0771$ ,  $wR2 = 0.1417$  (all data).

## Organic Field-Effect Transistors

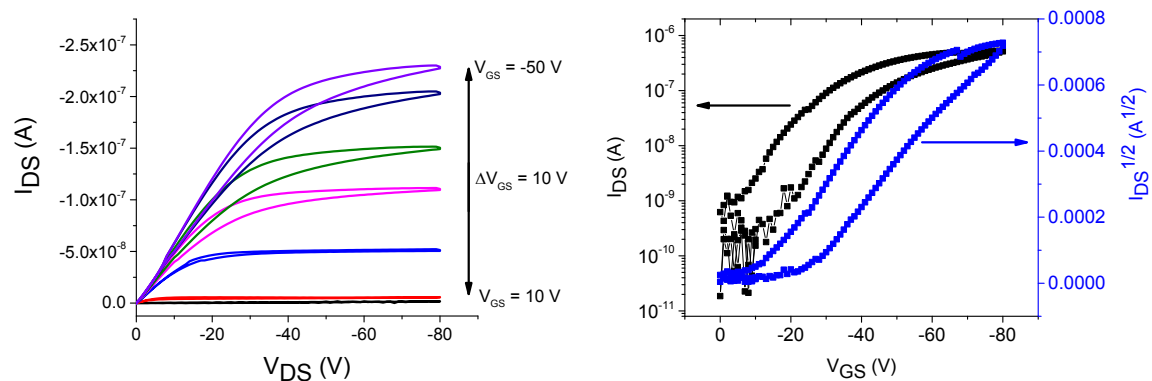


**Figure S8.** Output (left) and transfer ( $V_{DS} = -50$  V) (right) characteristics for OFETs containing BT-(TBF)<sub>2</sub>. Channel length = 10  $\mu$ m, width = 1 cm.

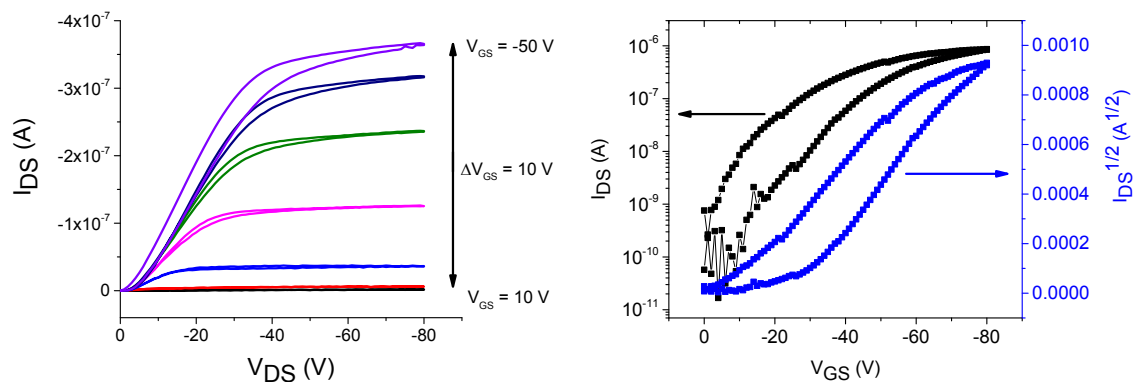


**Figure S9.** Output (left) and transfer ( $V_{DS} = -50$  V) (right) characteristics for OFETs containing BO-(TBF)<sub>2</sub>. Channel length = 10  $\mu$ m, width = 1 cm.

## Organic Photovoltaic Devices

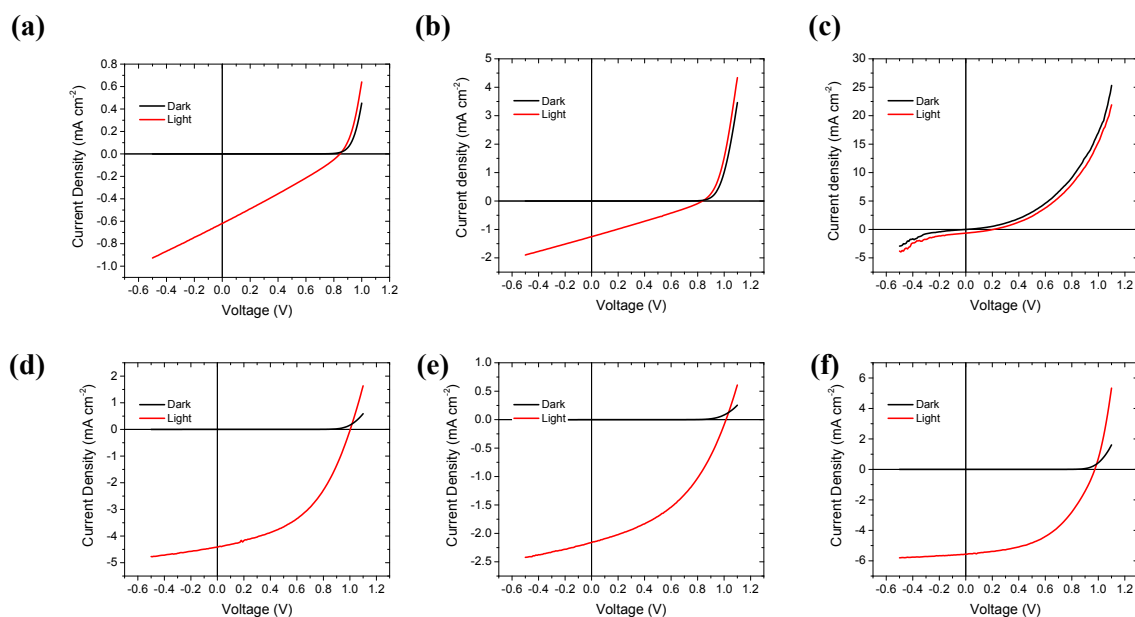


**Figure S10.** *J-V* characteristics for OPV devices fabricated with the following conditions: (a) **BT-(TBF)<sub>2</sub>** 1:2 PC<sub>61</sub>BM, unannealed; (b) **BT-(TBF)<sub>2</sub>** 1:2 PC<sub>61</sub>BM, annealed at 70°C; (c) **BT-(TBF)<sub>2</sub>** 1:2 PC<sub>61</sub>BM, annealed at 70°C, 1% DIO; (d) **BO-(TBF)<sub>2</sub>** 1:2 PC<sub>61</sub>BM, unannealed; (e) **BO-(TBF)<sub>2</sub>** 1:2 PC<sub>61</sub>BM, annealed at 70°C and (f) **BO-(TBF)<sub>2</sub>** 1:2 PC<sub>61</sub>BM, annealed at 70°C, 1% DIO.

## References

- 1 P. Ledwon, N. Thomson, E. Angioni, N. J. Findlay, P. J. Skabara and W. Domagala, *RSC Adv.*, 2015, **5**, 77303–77315.
- 2 I. Horcas, R. Fernández, J. M. Gómez-Rodríguez, J. Colchero, J. Gómez-Herrero and A. M. Baro, *Rev. Sci. Instrum.*, 2007, **78**, 13705.
- 3 S. J. Coles and P. A. Gale, *Chem. Sci.*, 2012, **3**, 683–689.
- 4 Rigaku Oxford Diffraction, *CrysAlisPro Version 1.171.39.9g*, 2016.
- 5 O. V. Dolomanov, L. J. Bourhis, R. J. Gildea, J. A. K. Howard and H. Puschmann, *J. Appl. Crystallogr.*, 2009, **42**, 339–341.
- 6 G. M. Sheldrick, *Acta Crystallogr. Sect. A Found. Crystallogr.*, 2015, **71**, 3–8.
- 7 G. M. Sheldrick, *Acta Crystallogr. Sect. C Struct. Chem.*, 2015, **71**, 3–8.
- 8 W. Yue, Y. Zhao, D. Song, H. Tian, Z. Xie, D. Yan, Y. Geng and F. Wang, *Macromolecules*, 2009, **42**, 6510–6518.